Am J Transl Res 2020;12(9):5064-5079
www.ajtr.org /ISSN:1943-8141/AJTR0117186

Original Article

Intramuscular accumulation of pentadecanoic acid activates AKT1 to phosphorylate NCOR1 and triggers FOXM1-mediated apoptosis in the pathogenesis of sarcopenia

Fa-Xiu Chen, Ning Du, Jian Hu, Fang Ning, Xun Mei, Qiang Li, Le Peng

Department of Geriatrics, Jiangxi Provincial People's Hospital Affiliated to Nanchang University, Nanchang 330006, Jiangxi, China

Received June 29, 2020; Accepted August 23, 2020; Epub September 15, 2020; Published September 30, 2020

Abstract: Sarcopenia is an age-associated disorder that results in skeletal muscle loss. Apoptosis and inflammation are the two major contributors to sarcopenia. Emerging evidence has shown that long-chain fatty acids (LCFAs) are implicated in the muscles of sarcopenic animal models. However, it is unknown whether LCFAs are correlated with apoptosis or inflammation in the pathogenesis of sarcopenia. Herein, we found that pentadecanoic acid (PDA), a C15 LCFA, was significantly accumulated in human sarcopenic muscles. *In vitro* PDA treatment could dose-dependently induce the expression of the transcription factor *FOXM1* (forkhead box M1) and several proapoptotic genes, such as *PUMA* (p53-upregulated modulator of apoptosis), *BAX* (B-cell/lymphoma 2-associated X) and *APAF1* (apoptotic peptidase activating factor 1), thereby causing apoptosis. Mechanically, PDA activated AKT1 (AKT serine/threonine kinase 1) to phosphorylate NCOR1 (nuclear receptor corepressor 1). The phosphorylated NCOR1 disassociated from the NCOR1-FOXM1 transcriptional complex and could not repress FOXM1-mediated transcription, leading to the induction of *PUMA*. The activated PUMA further triggered downstream apoptotic signaling, including activation of the BAX, APAF1 and caspase cascades, leading to the occurrence of apoptosis. Alkaline phosphatase or knockdown of *AKT1 in vitro* reversed the FOXM1-mediated apoptotic signaling. Collectively, our results provide new evidence that LCFAs are involved in the pathogenesis of sarcopenia by activating apoptotic signaling. Attempts to decrease the intake of PDA-containing foods or blocking AKT1 may improve the symptoms of sarcopenia.

Keywords: Sarcopenia, pentadecanoic acid, apoptosis, AKT1, FOXM1, NCOR1

Introduction

Sarcopenia, a disorder characterized by the degenerative loss of skeletal muscles, is prevalent in people over 65 years old. The epidemiology of sarcopenia in people 65-70 years old is nearly 14%, while it rises to over 50% in those over 80 years old [1, 2]. However, the etiopathogenetic mechanisms of sarcopenia are still not clearly defined. Sarcopenia is simply divided into two categories: primary sarcopenia and secondary sarcopenia [1]. Primary sarcopenia refers to patients who do not have other underlying medical problems, such as cardiovascular disease, diabetes, chronic respiratory disease or cancer, but are only experiencing aging itself [1, 3]. Apoptosis and inflammation are recognized as the two major contributors to the pathology of primary sarcopenia [1, 3]. Secondary sarcopenia is associated with the incidence of other diseases such as obesity, osteoporosis or type 2 diabetes [1, 3]. These sarcopenic patients often have a physical disability and a poor quality of life [1, 3]. Thus, in-depth research is urgently required to elucidate the pathogenic mechanisms of sarcopenia and discover strategies that can delay or even overcome sarcopenia.

Obesity is normally caused by the increased deposition of long-chain fatty acids (LCFAs) [4, 5]. The deposition of LCFAs in muscle can compromise muscle integrity [4, 5]. Because obesity is a risk factor for secondary sarcopenia,

some studies have investigated the roles of LCFAs in animal models of secondary sarcopenia [6-8]. Laurentius et al. found that LCFAs, such as linoleic acid, stearic acid, and vaccenic acid, and inflammatory markers, such as CCL2 (C-C motif chemokine ligand 2), CCL5, and CXCL2 (C-X-C motif chemokine ligand 2), were coaccumulated in the skeletal muscle of sarcopenic rats [6]. Other studies have found that LCFA accumulation in muscle can compromise protein anabolism and cause lipotoxicity, leading to low-grade inflammation [7, 8]. *In vitro* analyses indicated that LCFAs can directly induce the expression of cytokines [9]. However, it is unclear whether LCFAs can contribute to apoptosis in sarcopenic muscle. Recently, Chen et al. found that the accumulation of palmitic acid (PA), an LCFA, can induce apoptosis and inflammation in astrocytes in a Cav1 (caveolin 1) autophagic degradation-dependent manner [10]. Because of this important finding, together with the critical role of LCFAs in obesity, we speculate that LCFAs may contribute to the pathogenesis of sarcopenia through activating apoptosis.

Apoptosis can be stimulated by either external or internal signals and thus is divided into two pathways: the intrinsic and extrinsic apoptosis pathways [11]. The extrinsic pathway is mediated by death receptors such as Fas receptors, tumor necrosis factor receptors (TNFRs), and TNF-related apoptosis-inducing ligand (TRAIL) receptors [11, 12]. Once extracellular ligands such as TNF-α, FasL, and TRAIL bind to the death receptors, they further recruit adaptor proteins such as FADD (Fas-associated protein with death domain) and TRADD (TNFR1-associated DEATH domain protein) [11, 12]. The adaptor proteins initiate a series of downstream cascades, including Caspase 8 (CASP8) and CASP3/7/9, eventually resulting in apoptosis [11, 12]. The intrinsic pathway, also known as the mitochondrial pathway, is initiated by sensing intracellular stresses such as cell toxins, free radicals, DNA damage and viral infections [11, 12]. Upon sensing stress signals, cells activate a p53-dependent apoptotic pathway, causing the induction of p53-upregulated modulator of apoptosis (PUMA) [11-13]. The activated PUMA interacts with anti-apoptotic proteins such as Bcl-xL and Bcl-2, inhibiting their interactions with two pro-apoptotic proteins, BAX (BCL2 associated X) and BAK1 (BCL2 antagonist/killer 1) [11-13]. The activation of BAX and BAK1 induces mitochondrial outer membrane permeabilization (MOMP), causing the release of cytochrome *c*, which promotes CASP9 and APAF1 (apoptotic protease activating factor 1) to assemble the caspase-activating complex [11-13]. The apoptosome initiates caspase cascades, including CASP3 and CASP7, thereby advancing apoptosis. In addition to the p53-dependent activation of apoptotic signaling, a p53-independent pathway has also been identified in which the transcription factor FOXO3a (forkhead box O3a) can bind to the promoter of *PUMA* to mediate its expression [14-16]. The activation of autophagy can lead to the degradation of FOXO3a, thereby repressing the expression of *PUMA* and inhibiting PUMA downstream signaling [16]. Although the activation of apoptotic signaling in sarcopenic muscle was found many years ago, it is still unknown whether the p53-independent signaling also exists in this process.

To investigate whether LCFAs accumulate in human sarcopenic muscle, we measured their concentrations using gas chromatography-mass spectrometry (GC-MS). We found that pentadecanoic acid (PDA) was the LCFA with the highest muscle tissue concentration. We then performed a microarray analysis in cells treated with different doses of PDA to identify PDA-dependent genes. We found that *FOXM1* (forkhead box M1) and several proapoptotic genes such as *PUMA*, *BAX*, *BAK1* and *APAF1* were dose-dependently activated by PDA. We discovered a FOXM1 binding site in the promoter of *PUMA*. *In vitro* knockdown of *FOXM1* decreased the expression of *PUMA*, suggesting that *PUMA* was a target of FOXM1. We investigated how PDA activates FOXM1-mediated apoptotic signaling and explored the inhibition of this signaling *in vitro*. These findings may lead to future strategies for preventing the progression of sarcopenia *in vivo*.

Materials and methods

Sarcopenic muscle collection

A total of 24 paired quadriceps muscle tissue samples from young people without sarcopenia (Control) and older sarcopenic patients were used in this study. These quadriceps muscle tissues were the same samples that were used

in a previous study [17]. All participants were informed of the purpose of this study and signed a consent form that was reviewed by the Ethics Board of Jiangxi Provincial People's Hospital.

Measurement of LCFAs by GC-MS

The preparation of lipid fractions from the quadriceps muscle tissues and the measurement of LCFAs were conducted according to a previous protocol [6]. In brief, 50 mg of muscle tissue (n=10 for both control and sarcopenic tissues) was homogenized in 500 μL of PBS (Sigma-Aldrich, Shanghai, China, #806552), followed by adding 667 μL of chloroform (Sigma-Aldrich, #650498) and 333 μL of methanol (Sigma-Aldrich, #646377). The mixtures were vortexed for 1 min and then centrifuged at 13000 × g for 1 min. An SPE (solid phase extraction) column supplemented with 200 mg of dry silica gel (Sigma-Aldrich, #288624) was loaded with 100 mL of the chloroform layer. The LCFAs were eluted with 3 mL of 80% hexane/diethyl ether (Sigma-Aldrich, #270504 and #309966) and 4 mL of methanol. The elutes were thoroughly mixed with 2 mL of a 1% sulfuric acid (Sigma-Aldrich, #339741)/methanol mixture (v/v), followed by incubating at 50°C for 1 h. The resulting mixtures were incubated with 5% sodium chloride (Sigma-Aldrich, #S7653). The hexane layer was collected, and the individual LCFAs were measured by GC-MS according to a previous protocol [6].

Cell culture and transfection

The human skeletal muscle myoblast cell line HSMM-1 was purchased from Lonza (Basel, Switzerland, #CC2580). The cells were cultured in Dulbecco's modified Eagle's medium (DMEM) (Sigma-Aldrich, #D5546) containing 10% fetal bovine serum (FBS) (Sigma-Aldrich, #F4135) and 10 units of *antibiotic solution* (Sigma-Aldrich, #P4333). For gene overexpression (OE), cells were transfected with the following plasmids: pCDNA3-2 × Flag (empty vector), pCDNA3-2 × Flag-FOXM1, pCDNA3-2 × Flag-NCOR1 and pCDNA3-2 × Flag-AKT1. For gene knockdown (KD), cells were transfected with short hairpin RNA (shRNA) lentiviral transduction particles of individual genes, including *FOXM1* (#TRCN0000273939), *NCOR1* (#TRCN0000299677), and *AKT1* (#TRCN0000199889), using FuGene 6 (Roche Diagnostics Corp., Indianapolis, IN, USA, #E2691). The transfected cells recovered in DMEM for 6 h, followed by selection with medium containing 1 μg/mL puromycin for 48 h. The single puromycin-resistant cells were sorted for further culturing, followed by measuring the mRNA and protein levels of the target proteins.

Cell treatment with PDA

HSMM-1 cells at 80% confluence were treated with different concentrations (0, 0.1, 0.3 and 0.6 mM) of PDA (Sigma-Aldrich, #P6125) at 37°C for 12 h. The cells were then washed twice with PBS buffer, collected, and used in subsequent experiments.

Total RNA isolation, microarray and real-time quantitative PCR (RT-qPCR)

Total RNA was extracted from the PDA-treated cells, transfected cells and muscle tissues using TRIzol reagent (Sigma-Aldrich, #T9424) according to the manufacturer's protocol. After NanoDrop quantification, 1.0 μg of total RNA was applied to microarray analysis using a SurePrint G3 Human Gene Expression 8 × 60 K v2 Kit (Agilent Technologies, Santa Clara, CA, USA, #G4851B) following a previous protocol [17]. Briefly, total RNA samples were reversely transcribed into complementary DNAs (cDNAs) with a cDNA synthesis kit (Sigma-Aldrich, #11483188001), followed by fluorescent labeling with the SuperScript Plus Indirect cDNA Labeling System (Invitrogen, Shanghai, China, #L1014-05 and #L1014-06). The labeled cDNAs were fragmented and hybridized to the array chip at 45°C for 12 h, followed by washing to remove non-bound sequences. The fluorescent cDNAs were scanned using an iScan System (Illumina, San Diego, CA, USA, SY-101-1001). The differentially expressed genes were discovered by examining the hybridization intensity data with the iScan software (#20020824). For the RT-qPCR analyses, 500 ng of total RNA was subjected to reverse transcription to synthesize the first-strand cDNA. The individual gene expression level was examined by RT-qPCR with a SYBR Green PCR Kit (Sigma-Aldrich, #QR0100) using the primers listed in Supplementary Table 1. The PCR procedures and quantification method were as described previously [17].

Western blotting

The PDA-treated cells, transfected cells and muscle tissues were subjected to immunoblot analysis to determine protein levels using a previous protocol [17]. In brief, total cell extracts were obtained by lysing the cells and muscle tissues in RIPA (radioimmunoprecipitation assay) buffer (Sigma-Aldrich, #R0278) containing protease inhibitor (Sigma-Aldrich, #S8820). After centrifuging at 13000 × g for 15 min, the supernatant was quantified by NanoDrop. Equal amounts of total proteins were loaded onto 10% SDS-PAGE gels for separation, followed by transferring to PVDF (polyvinylidene difluoride) membranes. The membranes were blocked with 5% milk at room temperature for 1 h and then incubated at 4°C for 12 h with the following primary antibodies: anti-FOXM1 (Abcam, Cambridge, MA, USA, #ab207298), anti-PUMA (Abcam, #ab9643), anti-BAX (Sigma-Aldrich, #ZRB1103), anti-BAK1 (Thermo Fisher Scientific, Waltham, MA, USA, #MA5-32111), anti-CASP3 (Abcam, #ab4051), anti-CASP7 (Abcam, #ab181579), anti-CASP9 (Abcam, #ab25758), anti-BCL2 (Abcam, #ab196495), anti-FAS (Abcam, #ab82419), anti-BIM (Sigma-Aldrich, #B7929), anti-NCOR1 (Abcam, #ab58396), anti-AKT1 (Sigma-Aldrich, #SAB4300334), anti-Flag (Sigma-Aldrich, #F7425), anti-MYC (Sigma-Aldrich, #SAB4800447), and anti-GAPDH (Abcam, #ab9483). The membranes were then washed five times with TBST (tris-buffered saline with Tween 20), followed by incubating at room temperature for 1 h with the secondary antibodies anti-rabbit IgG (#ab6721) and anti-mouse IgG (#ab6728). After rinsing five times with TBST, the protein signals on the membrane were visualized using an ECL (enhanced chemiluminescence) kit (Sigma-Aldrich, #GERPN2016). The protein signal intensities were quantified with ImageJ software.

Immunoprecipitation (IP), mass spectrometry, and coimmunoprecipitation (Co-IP) assays

For the IP assay, equal weights (100 mg) of three sarcopenic muscle tissues were mixed and homogenized in 500 μL of RIPA buffer containing protease inhibitor. After centrifuging at 13000 × g for 15 min, 50 mL of supernatant was retained as input, while the remaining 450 mL of supernatant was immunoprecipitated with protein A agarose (Abcam, #ab193254) coated with anti-FOXM1. The purified FOXM1-associated complex was resolved on a 10% SDS-PAGE gel and then stained with a silver staining kit (Thermo Fisher Scientific, #24612). The positive protein bands were cut into ~1 mm slices and eluted with a trypsin kit (Thermo Fisher Scientific, #60109101), followed by mass spectrometry analysis. Meanwhile, the input and output proteins were subjected to western blotting to determine protein interactions. For the Co-IP assay, different combinations of plasmids, as indicated in the figures, were cotransfected into the HSMM-1 cells (1×10^7). After incubation at 37°C for 48 h, the cells were lysed in 400 μL of RIPA buffer containing protease inhibitor. The samples were then centrifuged at 13000 × g for 15 min, and 40 μL of supernatant was retained as input, while the remaining 360 μL of supernatant was immunoprecipitated with anti-Flag agarose (Sigma-Aldrich, #A4596) and anti-MYC agarose (Sigma-Aldrich, #A7470). The input and output proteins were subjected to western blotting to determine protein interactions.

Chromatin immunoprecipitation (ChIP) assay

Cells (~1×10^8) were rinsed twice with PBS buffer, followed by crosslinking with 1% formaldehyde/PBS (v/v) at room temperature for 15 min. The cells were then collected and subjected to ChIP procedures using a kit (Sigma-Aldrich, #17-295) following the manufacturer's method. The purified DNA samples were used for RT-qPCR analysis with the following primers: forward: 5'-AGGCAGTCCACGCACCTTGGCC-3'; reverse: 5'-CACAGGGGACACACACATACACA-3'.

Luciferase assay

The wild-type (WT) promoter of *PUMA* was cloned into the pGL3 firefly vector. Using pGL3-pPUMA^{WT} as the template, we generated its two mutants [deletions of the two potential FOXM1 binding sites (BS)], termed pGL3-pPUMA$^{\triangledown\text{-}830\text{-}838}$ (BS1) and pGL3-pPUMA$^{\triangledown\text{-}982\text{-}990}$ (BS2). These three vectors were cotransfected with Renilla into Control-KD, FOXM1-KD1, FOXM1-KD2, Control-OE and FOXM1-OE cells. After incubating at 37°C for 24 h, the cells were applied to a luciferase assay using a Dual-

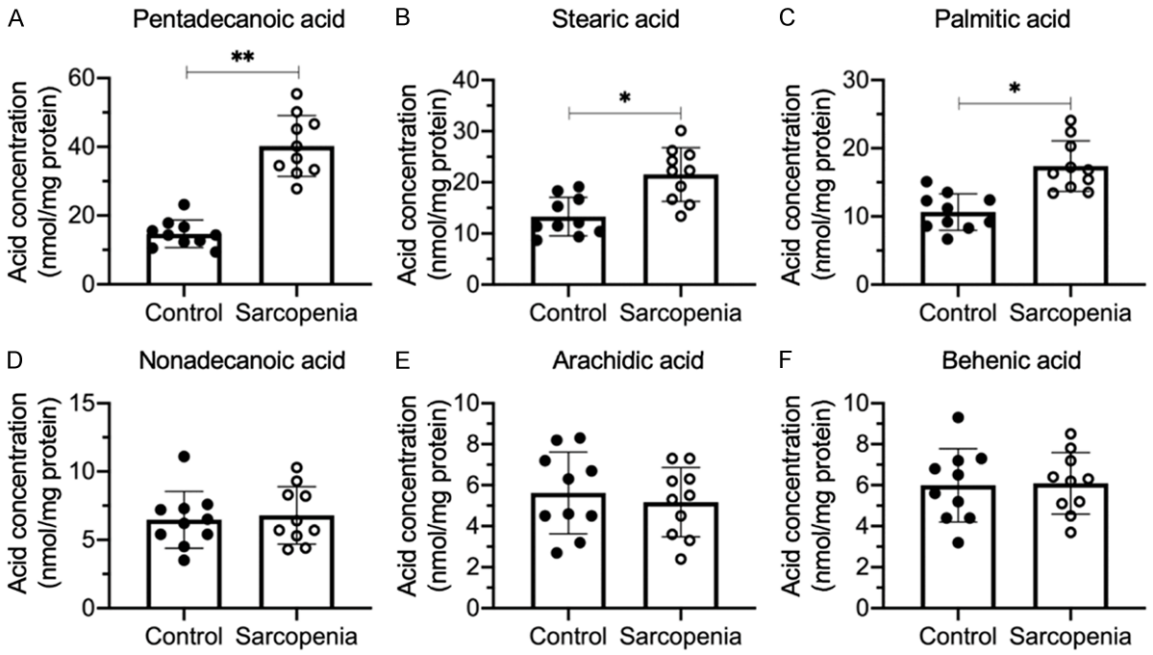

Figure 1. The accumulation of LCFAs in the quadriceps muscles from sarcopenia patients. LCFAs were extracted from non-sarcopenic (Control) and sarcopenic tissues (n=10 for each group). The LCFA concentrations were measured in the hexane layer mixture using GC-MS and included PDA (A), stearic acid (B), palmitic acid (C), nonadecanoic acid (D), arachidic acid (E) and behenic acid (F). Statistical significance was denoted by * for $P<0.05$ and *** for $P<0.001$.

Luciferase Report Assay Kit (Promega, Madison, WI, USA, #E1910) following the protocol provided by the manufacturer.

Statistical analysis

Except for the microarray analysis, all other experiments were performed in triplicate independently. The data were analyzed using SPSS software (version 22) to determine the mean ± standard deviation (SD) using two-sided Student's *t* tests. The significance levels are presented as $P>0.05$ (no significance, ns), $P<0.05$ (*), $P<0.01$ (**) and $P<0.001$ (***).

Results

PDA was significantly accumulated in sarcopenic muscle tissues

Previous studies in sarcopenic animal models have shown that the LCFAs, such as linoleic acid, stearic acid and vaccenic acid, accumulate in obese sarcopenic animals [6]. In a recent publication from our group, we collected 24 muscle tissues from sarcopenic patients and found that apoptotic signaling was activated [17]. To determine whether the LCFA concentrations were changed in our samples, we randomly selected 10 paired nonsarcopenic and sarcopenic tissues, extracted the LCFAs, and then measured their concentrations by GC-MS. We discovered that three LCFAs, PDA (C15), stearic acid (C17) and palmitic acid (C16), were accumulated in the sarcopenic muscle tissues compared to nonsarcopenic muscles (**Figure 1A-C**). Of these LCFAs, PDA showed the most significant increase (~2.3-fold increase) (**Figure 1A**), while stearic acid and palmitic acid increased by only ~1.5-fold in the sarcopenic tissues (**Figure 1B** and **1C**). In addition, we also identified unchanged concentrations of three other LCFAs: nonadecanoic acid (C19), arachidic acid (C20) and behenic acid (C22) (**Figure 1D-F**). The chemical structures of these six LCFAs are shown in Supplementary Figure 1. The substantial differences between our current results from human sarcopenic patients and previous results from animal sarcopenic muscles suggest that the LCFA distributions found among various species and pathological conditions might differ considerably. Because PDA showed the most significant accumulation in sarcopenic muscle tissues, we further investigated its molecular effects.

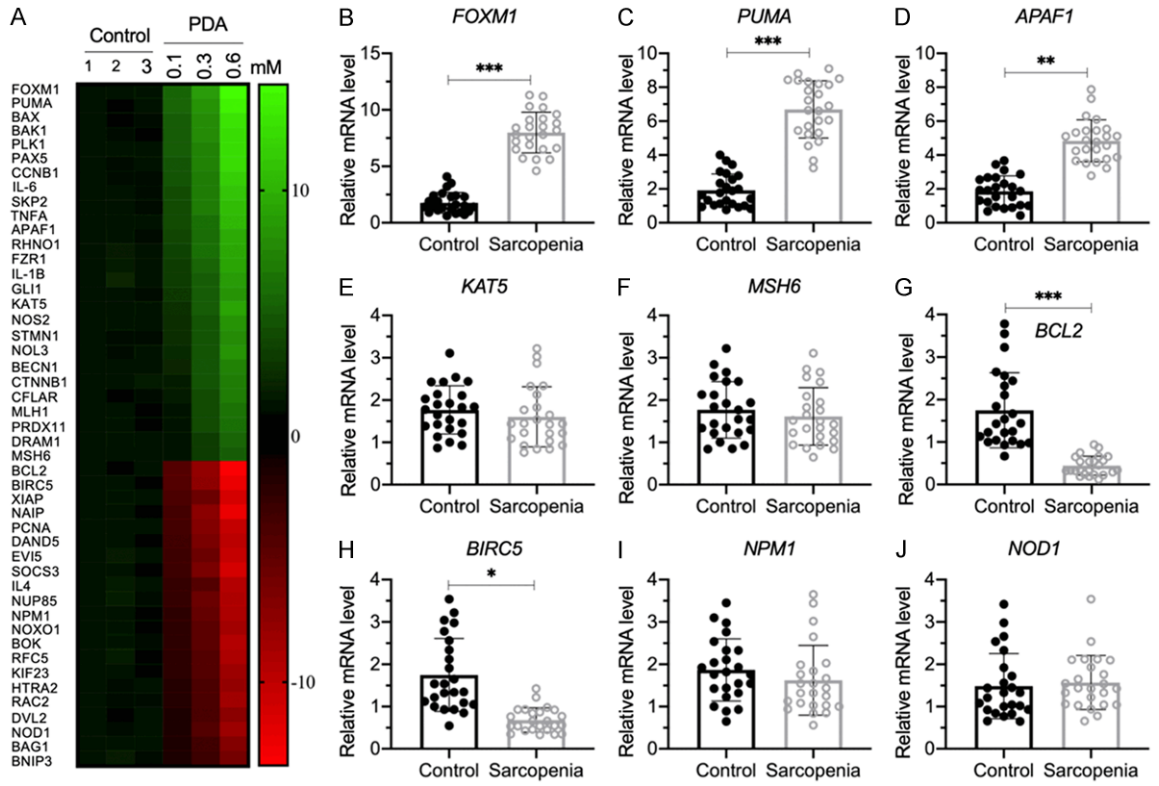

Figure 2. The identification of aberrantly expressed genes in PDA-treated cells and verification of nine representative gene expression levels in human sarcopenic muscles. (A) The heat map of differentially expressed genes. HSMM-1 cells were treated with different doses of PDA (0, 0.1, 0.3 and 0.6 mM) for 12 h, followed by RNA isolation and microarray analysis. The differentially expressed genes that were dose-dependent on PDA are shown. (B-J) Detection of nine representative gene expression levels by RT-qPCR. Nine representative genes, including *FOXM1* (B), *PUMA* (C), *APAF1* (D), *KAT5* (E), *MSH6* (F), *BCL2* (G), *BIRC5* (H), *NPM1* (I) and *NOD1* (J), were selected to examine their expression levels in the nonsarcopenic (Control) and sarcopenic tissues (n=24 for each). Statistical significance was denoted by * for $P<0.05$, ** for $P<0.01$, and *** for $P<0.001$.

PDA induced the expression of FOXM1 and proapoptotic genes in vitro

To determine whether PDA could alter the gene expression levels, we treated HSMM-1 cells with a series of PDA doses (0, 0.1, 0.3 and 0.6 mM) and performed a microarray analysis to examine differentially expressed genes. As presented in **Figure 2A**, we discovered 47 PDA-dependent genes, including 26 upregulated genes and 21 downregulated genes after PDA treatment. Among these upregulated genes, we observed the transcription factor-encoding gene *FOXM1* and several proapoptotic genes, including *PUMA*, *BAX*, *BAK1* and *APAF1* (**Figure 2A**). Moreover, we also observed several proinflammatory cytokine genes, including *IL-6* (interleukin 6), *IL1B* (interleukin 1-beta), and *TNFA* (tumor necrosis factor-alpha) (**Figure 2A**). In contrast, we found that several anti-apoptotic genes, such as *BCL2*, *BIRC5* (baculoviral IAP repeat-containing 5) and *XIAP* (X-linked inhibitor of apoptosis) were downregulated after PDA treatment (**Figure 2A**). These results suggested that PDA might induce apoptosis and inflammation *in vitro*, which were recognized as two important causes of sarcopenia pathogenesis. To examine whether genes identified in the microarray results were also dysregulated in sarcopenic muscle tissues, we randomly selected five upregulated genes, including *FOXM1*, *PUMA*, *APAF1*, *KAT5* (lysine acetyltransferase 5) and *MSH6* (MutS homolog 6), and four downregulated genes, including *BCL2*, *BIRC5*, *NPM1* (nucleophosmin 1) and *NOD1* (nucleotide binding oligomerization domain containing 1), and performed RT-qPCR to measure their expression levels in the 24 paired muscle tissues. The expression levels of *FOXM1*, *PUMA* and *APAF1* were shown

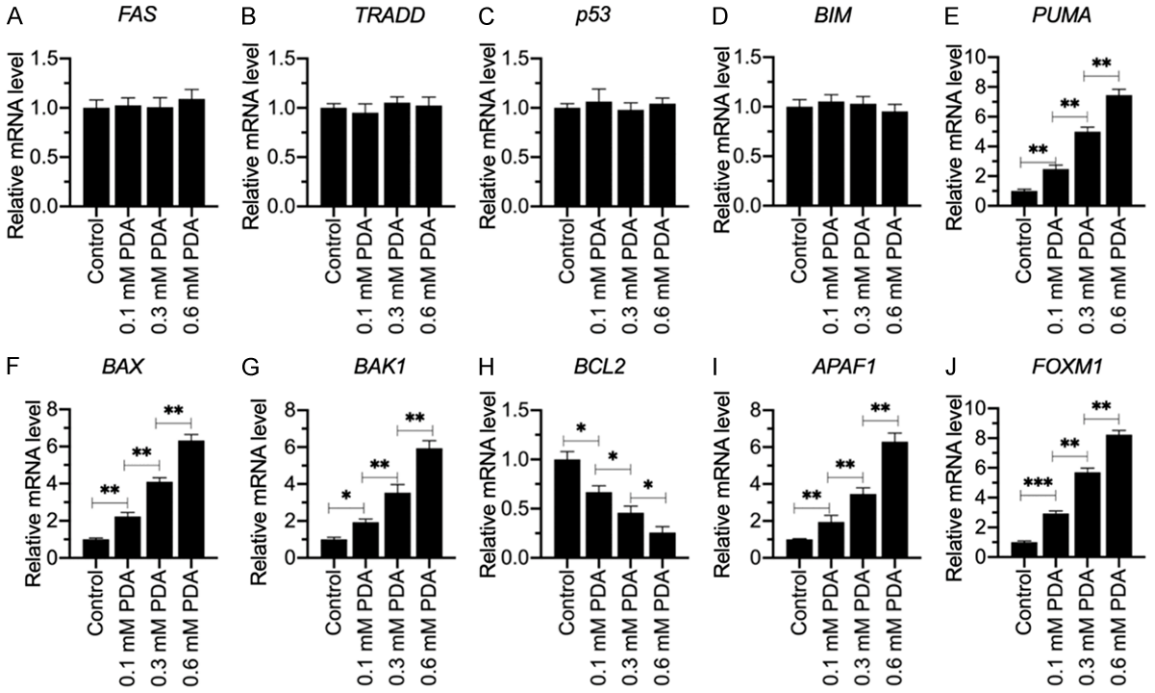

Figure 3. The mRNA levels of genes involved in apoptotic signaling in PDA-treated cells. Total RNA samples from cells treated with different doses of PDA (0, 0.1, 0.3 and 0.6 mM) were examined for their mRNA levels of *FAS* (A), *TRADD* (B), *p53* (C), *BIM* (D), *PUMA* (E), *BAX* (F), *BAK1* (G), *BCL2* (H), *APAF1* (I) and *FOXM1* (J) by RT-qPCR. Statistical significance was denoted by * for $P<0.05$, ** for $P<0.01$, and *** for $P<0.001$.

to be upregulated in sarcopenic tissues compared to controls (**Figure 2B-D**). However, we did not observe a significant change in the expression of *KAT5* and *MSH6* (**Figure 2E** and **2F**). In addition, in sarcopenic tissues, we found a significant decrease in *BCL2* and *BIRC5* but not in *NPM1* or *NOD1* compared to controls (**Figure 2G-J**).

The induction of proapoptotic genes and the reduction of anti-apoptotic genes in sarcopenic tissues suggested that apoptosis signaling pathways were activated in the pathogenesis of sarcopenia and in the PDA-treated cells. To explore which apoptosis signaling pathways were activated by PDA treatment, we examined the mRNA and protein levels of two extrinsic molecules, including FAS and TRADD, and three intrinsic molecules, including p53, BIM and PUMA, in cells treated with different doses of PDA. Our results showed that the mRNA and protein levels of FAS, TRADD, p53 and BIM were not affected by PDA treatment (**Figure 3A-D**, Supplementary Figure 2A and 2B). In contrast, PDA treatment resulted in a dose-dependent induction of PUMA (**Figure 3E**, Supplementary Figure 2A and 2B). These results suggested that the activation of PUMA after PDA treatment might be independent of p53. Moreover, we also examined the expression levels of several *PUMA* downstream genes in intrinsic signaling, including *BCL2*, *BAX*, *BAK1* and *APAF1*. The RT-qPCR and western blotting results indicated that *BCL2* expression was dose-dependently repressed by PDA, while the other three molecules were dose-dependently induced by PDA (**Figure 3F-I**, Supplementary Figure 2A and 2B). These results suggested that PDA could activate intrinsic apoptosis signaling through a p53-independent mechanism. To further confirm the activation of intrinsic apoptosis signaling, we also determined the protein levels of CASP3, -7 and -9. Consistent with the induction patterns of PUMA, BAX, BAK1 and APAF1, we also found these three caspases to be dose-dependently induced by PDA (Supplementary Figure 2A and 2C). Several studies have shown that the transcription factor FOXO3a can control the expression of *PUMA* in a p53-independent manner [15, 16]. Additionally, FOXM1, a homolog of FOXO3a,

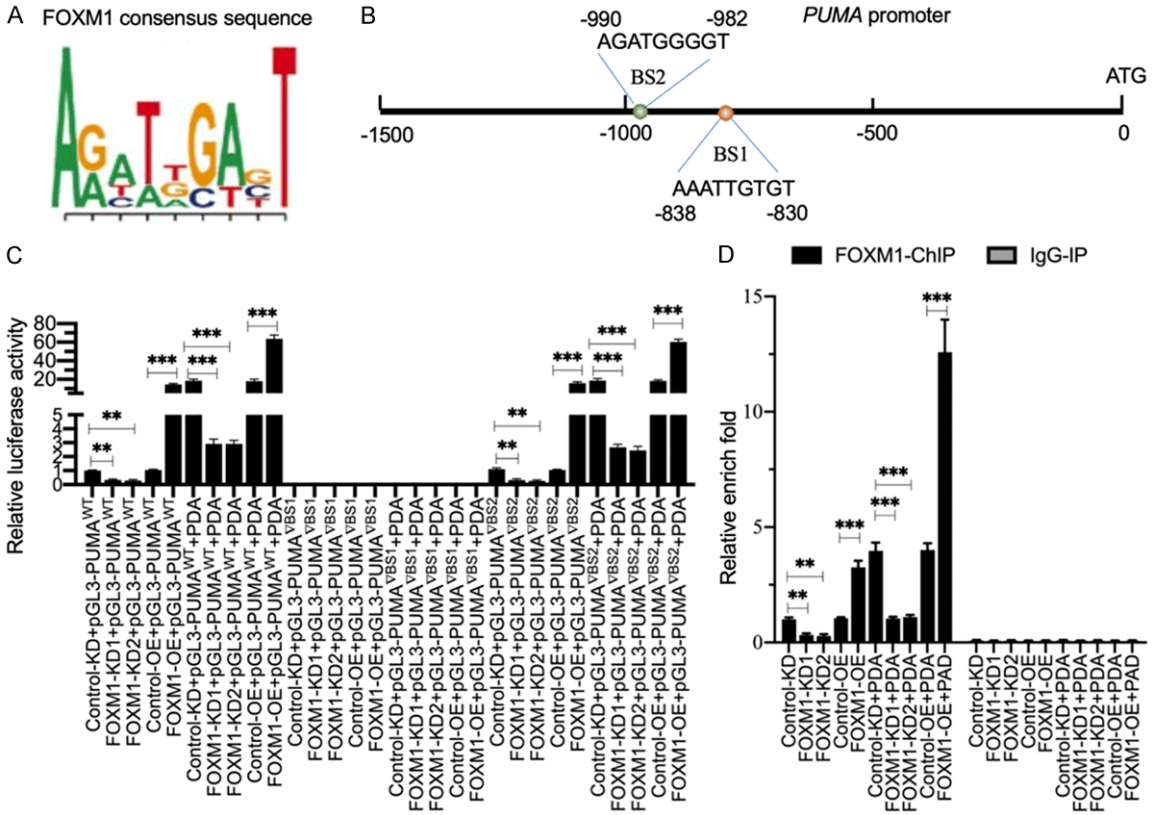

Figure 4. FOXM1 docked onto the promoter of *PUMA* at the BS1 site to regulate its expression. A. The consensus sequence of FOXM1. B. The promoter of *PUMA* contained two putative FOXM1 binding sites. A 1500-bp length of the *PUMA* promoter was assessed for FOXM1 binding sites. Two binding sites (BS1 and BS2) were identified; their positions were shown. C. The relative luciferase activities. Three plasmids, pGL4.3-pPUMA^{WT}, pGL4.3-pPUMA$^{\triangledown BS1}$ and pGL4.3-pPUMA$^{\triangledown BS2}$, were cotransfected with Renilla into Control-KD, FOXM1-KD1, FOXM1-KD2, Control-OE and FOXM11-OE cells. The transfected cells were cultured for an additional 24 h and then subjected to a dual-luciferase reporter assay. The relative luciferase activities were determined by normalizing the firefly luciferase activities to their corresponding Renilla activities. ***P*<0.01 and ****P*<0.001. D. The occupancy of FOXM1 on the promoter of *PUMA*. The ChIP assays were performed in Control-KD, FOXM1-KD1, FOXM1-KD2, Control-OE and FOXM1-OE cells using anti-FOXM1 and IgG (negative control). The purified input and output DNA samples were subjected to RT-qPCR analysis to examine the occupancy of FOXM1 on the promoter of *PUMA*. ***P*<0.01 and ****P*<0.001.

showed an induction pattern similar to that of PUMA after PDA treatment (**Figure 3E** and **3J**, Supplementary Figure 2A-C). These results suggested that the expression of *PUMA* and its downstream signaling might be controlled by FOXM1.

FOXM1 regulated the expression of PUMA at the transcriptional level

To determine whether FOXM1 has a regulatory mechanism towards *PUMA* expression similar to that of FOXO3a, we first generated FOXM1 knockdown and overexpression cell lines and then examined the effects of FOXM1 repression and induction on *PUMA* expression. As shown in Supplementary Figure 3, knockdown of *FOXM1* decreased the levels of *PUMA* mRNA and protein, while its overexpression resulted in the opposite effect. We then scanned the FOXM1 binding sites using its consensus sequence in the promoter of *PUMA* (**Figure 4A**). In a 1500-bp length of the *PUMA* promoter, we found two potential FOXM1 binding sites, AAATTGTGT located at -830-(-)838 (BS1) and AGATGGGGT located at -982-(-)990 (BS2) (**Figure 4B**). To determine the necessity of these two sites for FOXM1 binding, we constructed vectors containing the WT promoter (pGL3-pPUMA^{WT}) and deletions of these two sites (pGL3-pPUMA$^{\triangledown BS1}$ and pGL3-pPUMA$^{\triangledown BS2}$). These plasmids were transfected into FOXM1-KD and FOXM1-OE cells. After treating with or without 0.3 mM PDA, the cells were subjected

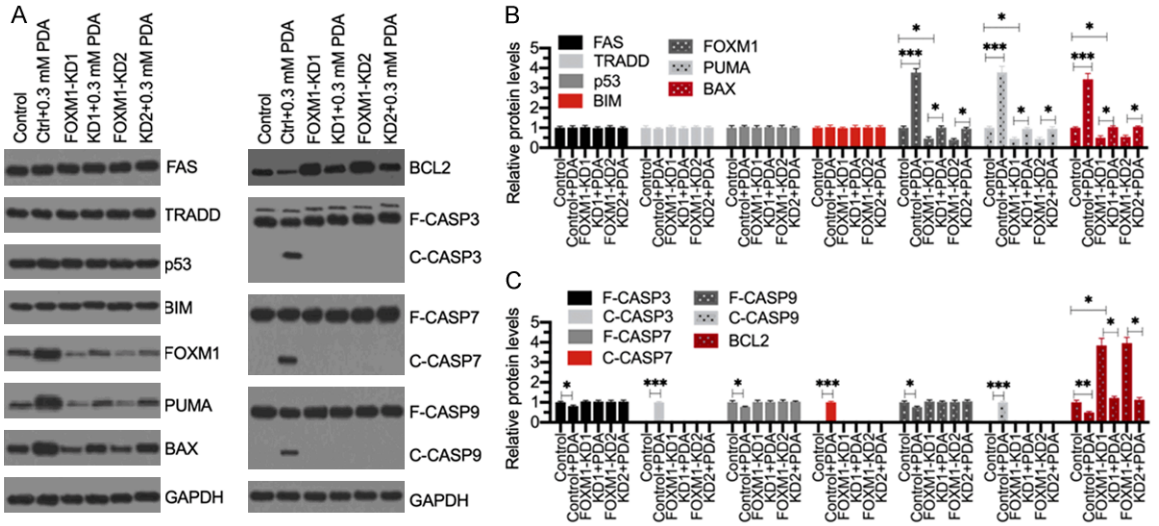

Figure 5. Knockdown of *FOXM1* failed to active apoptosis signaling following PDA treatment. (A) Western blotting results. The Control-KD (Control), FOXM1-KD1 and FOXM1-KD2 cells were treated with or without 0.3 mM PDA for 12 h, followed by total protein extraction. Western blotting analyses were performed to detect the protein levels of FAS, TRADD, p53, BIM, FOXM1, PUMA, BAX, BCL2, CASP3, CASP7, CASP9, and GAPDH (loading control). (B and C) The normalized protein levels. The protein signals as shown in (A) were quantified using ImageJ software and then normalized to their corresponding GAPDH levels. ***P*<0.05, ***P*<0.01 and ****P*<0.001.

to luciferase assay. Our results showed that knockdown of *FOXM1* repressed luciferase activity, but its overexpression increased luciferase activity in cells transfected with pGL3-pPUMA^{WT} (**Figure 4C**). The deletion of the BS1 site on the promoter of *PUMA* resulted in the disappearance of luciferase signal in all cell lines (**Figure 4C**). In contrast, cells transfected with pGL3-pPUMA$^{\triangledown BS2}$ had the same pattern of luciferase activity as those transfected with the WT promoter (**Figure 4C**). These results suggested that only BS1 was necessary for FOMX1 binding to the promoter of *PUMA*. We also observed that PDA treatment significantly induced the luciferase activity in cells cotransfected with the pGL3-pPUMA^{WT} and pGL3-pPUMA$^{\triangledown BS2}$ vectors (**Figure 4C**). These results suggested that FOXM1 could bind to the promoter of *PUMA* to regulate its expression, and the induction of *PUMA* following PDA treatment was dependent on FOXM1. In addition, we performed ChIP assays using anti-FOXM1 and IgG (negative control) to determine whether FOXM1 could directly bind to the promoter of *PUMA*. Our results indicated that FOXM1 binding to the promoter of *PUMA* was significantly repressed following *FOXM1* knockdown but was markedly increased upon *FOXM1* overexpression (**Figure 4D**). PDA treatment intensified these effects and increased the occupancy of FOXM1 on the promoter of *PUMA* (**Figure 4D**).

PDA failed to activate apoptosis signaling in FOXM1-KD cells

The above results showed that PDA dose-dependently induced intrinsic molecules (see **Figure 3** and Supplementary Figure 2). To determine whether their activation was dependent on FOXM1, we treated Control-KD and FOXM1-KD cells with 0.3 mM PDA and then examined the protein levels of intrinsic molecules. As shown in **Figure 5A** and **5B**, *FOXM1* knockdown did not change the protein levels of FAS, TRADD, p53 or BIM. By contrast, *FOXM1* downregulation resulted in a significant reduction in proapoptotic proteins, including PUMA, BAX, BAK1 and APAF1, and induced the anti-apoptotic protein BCL2. After PDA treatment, these proapoptotic proteins were induced to levels comparable to those in Control-KD cells without PDA treatment, but the levels were much lower than those of Control-KD cells treated with PDA (**Figure 5A** and **5B**). Importantly, PDA failed to activate CASP3, -7 and -9 in FOXM1-KD cells (**Figure 5A** and **5C**), suggesting that the activation of apoptosis signaling by PDA treatment is dependent on FOXM1.

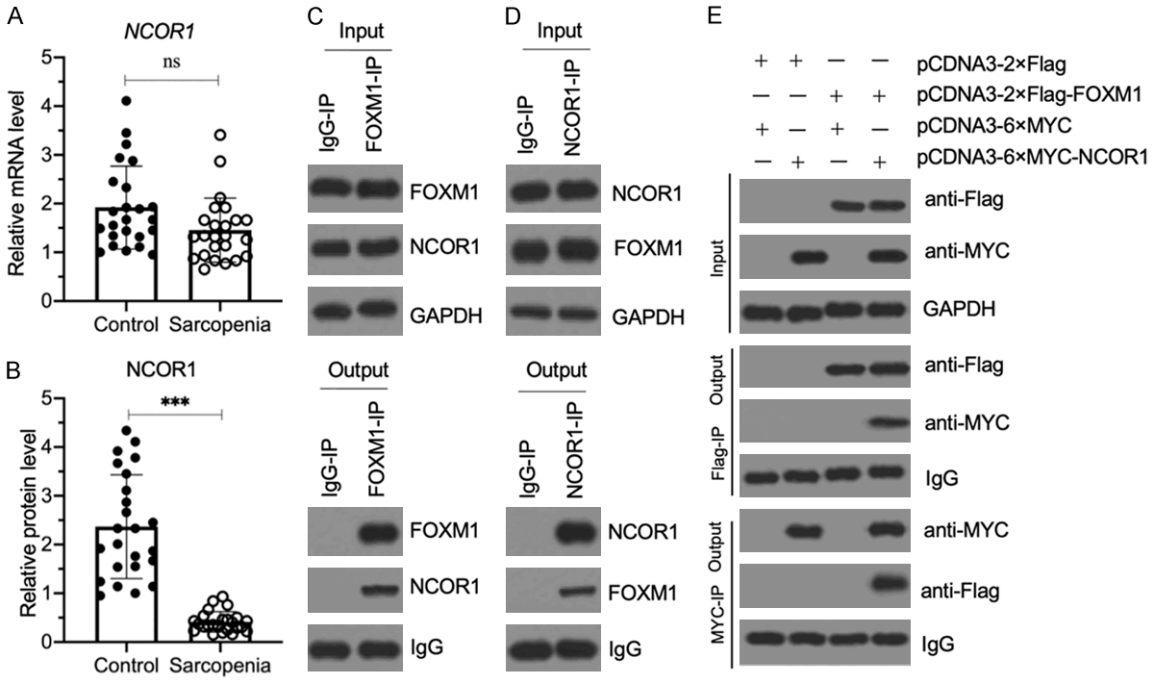

Figure 6. NCOR1 assembled a transcriptional complex with FOXM1. (A) The relative *NCOR1* mRNA level in sarcopenic muscles. The same RNA samples as used in **Figure 2B** were applied to RT-qPCR analyses to examine the *NCOR1* mRNA level. $P>0.05$ (ns indicates no significance). (B) The relative NCOR1 protein level in sarcopenic muscles. The same muscle tissues as in (A) were used to extract total proteins, and the cell extracts were subjected to immunoblotting to examine NCOR1 and GAPDH (loading control) protein. The relative NCOR1 protein level was determined by normalizing to its corresponding GAPDH level. ***$P<0.001$. (C and D) FOXM1 and NCOR1 could pull down each other *in vivo*. Equal weights of three sarcopenic tissues were mixed together, and their homogenates were subjected to IP assays with IgG, anti-FOXM1 (C) and anti-NCOR1 (D), respectively. The input and output proteins were examined for their FOXM1 and NCOR1 protein levels by western blotting. (E) FOXM1 directly interacted with NCOR1 *in vitro*. The HSMM-1 cells were cotransfected with the plasmid combinations shown in the figure. After culturing for 48 h, the cells were used for Co-IP assays with Flag-agarose and MYC-agarose. The input and output proteins were examined by western blot for their protein levels using anti-Flag and anti-MYC antibodies.

FOXM1 assembled a transcriptional complex with NCOR1 to mediate the expression of PUMA

Transcription factors typically assemble transcriptional complexes with other regulatory proteins, such as corepressors and coactivators [18]. To investigate the transcriptional complex members associated with FOXM1, we performed an IP assay with the homogenized mixture of three sarcopenic muscle tissues using anti-FOXM1 antibody. The purified FOXM1-associated complex was subjected to mass spectrometry analysis. We obtained 53 potential candidate proteins, one of which was the corepressor NCOR1 (Supplementary Table 2). We then examined the mRNA and protein levels of NCOR1 in the 24 paired muscle tissues. The level of *NCOR1* mRNA was not significantly changed in the sarcopenic tissues compared to controls (**Figure 6A**). However, NCOR1 protein was dramatically decreased in the sarcopenic tissues (**Figure 6B**). Owing to the important role of NCOR1 in coordinating transcription factors to regulate gene expression, we next sought to determine whether NCOR1 could form a complex with FOXM1. First, we examined the input and output proteins used for mass spectrometry analysis. The western blotting results showed that FOXM1 could pull down NCOR1 *in vivo* (**Figure 6C**). Second, we performed an IP assay with the same homogenized mixture with anti-NCOR1 antibody, and we also found that NCOR1 could pull down FOXM1 *in vivo* (**Figure 6D**). Finally, we investigated the direct interaction between FOXM1 and NCOR1 in cells cotransfected with pCDNA3-2 × Flag-FOXM1 and pCDNA3-6 × MYC-NCOR1. The Co-IP assay results showed that FOXM1 could directly interact with NCOR1 (**Figure 6E**).

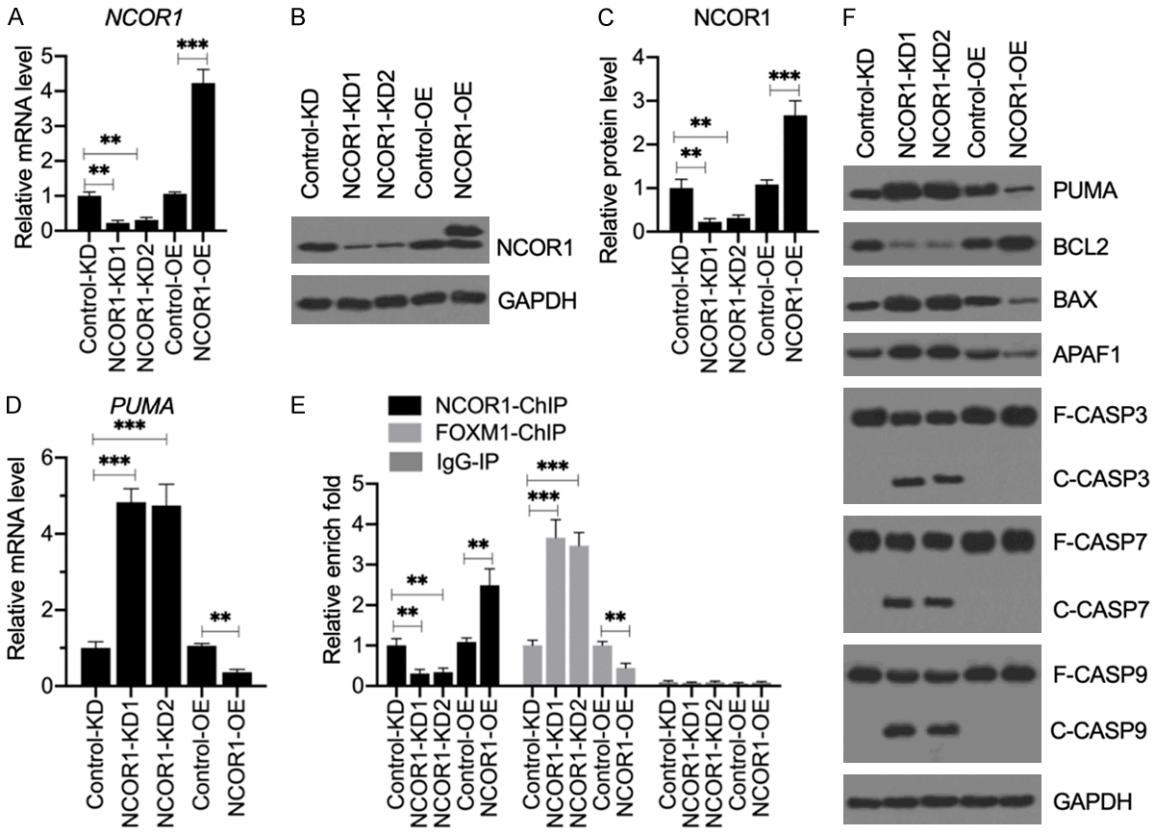

Figure 7. Knockdown of *NCOR1* activated apoptosis signaling without PDA treatment. (A) The relative mRNA level of *NCOR1*. Total RNA from Control-KD, NCRO1-KD1, NCOR1-KD2, Control-OE and NCOR1-OE cells was applied to RT-qPCR analysis to examine *NCOR1*. mRNA levels $^{**}P<0.01$ and $^{***}P<0.001$. (B and C) NCOR1 protein levels. Total cell extracts from the cells used in (A) were applied to western blotting to examine the protein levels of NCOR1 and GAPDH (loading control) (B). The NCOR1 protein signals were quantified using ImageJ software and normalized to their corresponding GAPDH levels (C). $^{**}P<0.01$ and $^{***}P<0.001$. (D) The relative *PUMA* mRNA level. The same RNA samples as used in (A) were subjected to RT-qPCR analysis to examine the *PUMA* expression. $^{**}P<0.01$ and $^{***}P<0.001$. (E) The occupancy of NCOR1 and FOXM1 on the promoter of *PUMA*. ChIP assays were performed in Control-KD, NCOR1-KD1, NCOR1-KD2, Control-OE and NCOR1-OE cells using anti-NCOR1, anti-FOXM1 and IgG (negative control). The purified input and output DNA samples were subjected to RT-qPCR analysis to examine the occupancy of NCOR1 and FOXM1 on the promoter of *PUMA*. $^{**}P<0.01$ and $^{***}P<0.001$. (F) The effects of *NCOR1* knockdown on apoptotic proteins. Cells used in (A) were subjected to western blotting to examine the protein levels of PUMA, BCL2, BAX, APAF1, CASP3, CASP7, CASP9, and GAPDH (loading control).

NCOR1 negatively regulated the expression of PUMA

Since NCOR1 is a corepressor and our results in **Figure 6B** show that NCOR1 protein was significantly decreased in sarcopenic muscle tissues, we speculated that NCOR1 might negatively control the expression of *PUMA*. To verify this hypothesis, we first generated NCOR1 knockdown and overexpression cell lines (**Figure 7A-C**) and then measured *PUMA* mRNA levels in these cells. As expected, the RT-qPCR results showed that knockdown of *NCOR1* caused a significant increase of *PUMA* mRNA, while the overexpression of *NCOR1* resulted in *PUMA* downregulation (**Figure 7D**). We then performed a ChIP assay in PUMA-KD and PUMA-OE cells using anti-NCOR1, anti-FOXM1 and IgG to determine the occupancies of NCOR1 and FOXM1 on the promoter of P*UMA*. The occupancy of NCOR1 on the promoter of *PUMA* was similar to its mRNA expression level patterns (**Figure 7E**). In contrast, we found that the occupancy of FOXM1 was significantly increased in NCOR1-KD cells but dramatically decreased in NCOR1-OE cells (**Figure 7E**). These results suggested that NCOR1 functions as a repressor of FOXM1 to regulate *PUMA*

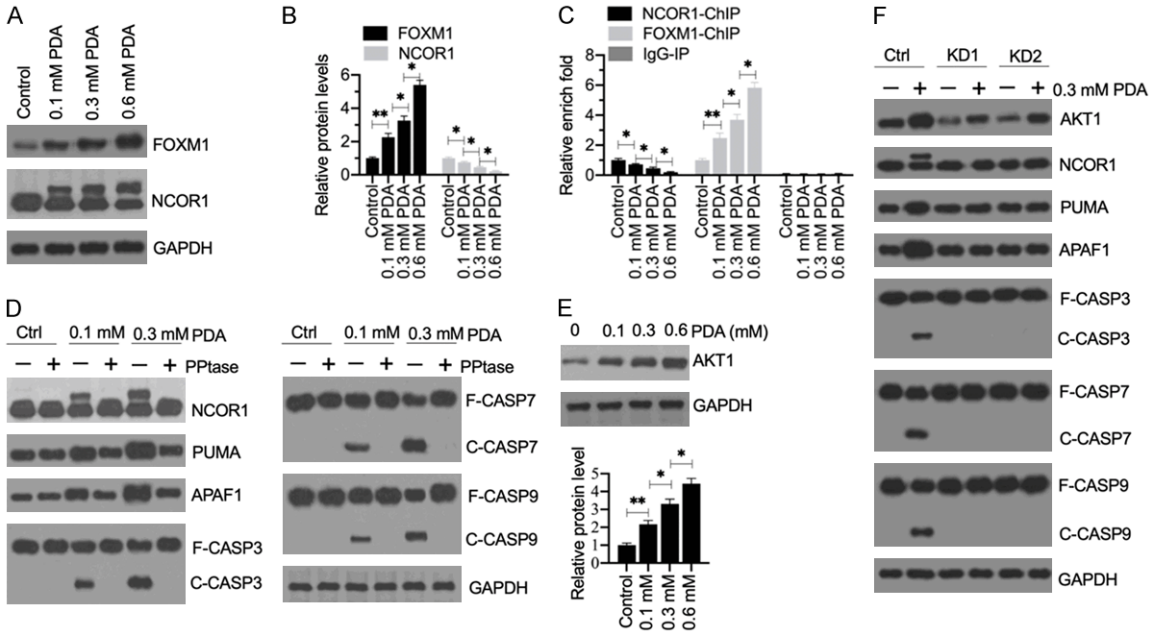

Figure 8. The phosphorylation of NCOR1 mediated by AKT1 was required for the activation of apoptosis signaling. (A) The protein levels of FOXM1 and NCOR1 in PDA-treated cells. Total cell extracts from cells treated with different doses of PDA (0, 0.1, 0.3 and 0.6 mM) were subjected to western blotting to examine the protein levels of FOXM1, NCOR1, and GAPDH (loading control). (B) Quantification of protein band signals. The protein band signals in (A) were quantified using ImageJ software. **P*<0.05 and ***P*<0.01. (C) The occupancy of NCOR1 and FOXM1 on the promoter of *PUMA*. ChIP assays were performed in the cells used in (A) with anti-NCOR1, anti-FOXM1 and IgG (negative control). The purified input and output DNA samples were subjected to RT-qPCR analysis to examine the occupancy of NCOR1 and FOXM1 on the promoter of *PUMA*. ***P*<0.05 and ***P*<0.01. (D) The effect of phosphatase (PPtase) on NCOR1 and apoptotic proteins. HSMM-1 cells were treated with or without 0.1 and 0.3 mM PDA for 12 h, followed by treating with or without PPtase for 2 h. Total protein extracts were subjected to western blotting to examine the protein levels of NCOR1, PUMA, APAF1, CASP3, CASP7, CASP9, and GAPDH (loading control). (E) The protein levels of AKT1 in PDA-treated cells. The same protein samples as used in (A) were subjected to western blotting to examine the protein levels of AKT1 and GAPDH (loading control). The protein signals were quantified. (F) The effect of AKT1 knockdown on apoptotic proteins. Control-KD (Ctrl), AKT1-KD1 (KD1) and AKT1-KD2 (KD2) cells were treated with or without 0.3 mM PDA for 12 h. Total protein extracts were subjected to western blotting to examine the protein levels of AKT1, NCOR1, PUMA, APAF1, CASP3, CASP7, CASP9, and GAPDH (loading control).

expression. In addition, we examined the protein levels of PUMA, BCL2, BAX, APAF1, CASP3, CASP7 and CASP9 in NCOR1-KD and NCOR1-OE cells. The immunoblot results indicated that *NCOR1* knockdown resulted in the significant accumulation of proapoptotic proteins but reduced the level of BCL2 (**Figure 7F** and Supplementary Figure 4). The three caspases were also activated in NCOR1-KD cells, suggesting that knockdown of *NCOR1* could activate apoptosis signaling.

PDA activated AKT1 (AKT serine/threonine kinase 1) to phosphorylate NCOR1

The above result in **Figure 6B** indicated that the NCOR1 protein level was decreased in sarcopenic muscle tissues. We next aimed to explore whether its decrease was controlled by PDA. For this purpose, we first examined the NCOR1 protein level in PDA-treated cells. As shown in **Figure 8A** and **8B**, we observed a dose-dependent decrease in the NCOR1 protein level after the PDA treatment. In addition, we examined the occupancies of NCOR1 and FOXM1 on the promoter of *PUMA* after treatment with the different PDA doses. The ChIP results showed that the NCOR1 occupancy gradually decreased with increasing PDA concentration, and this trend was reversed for the FOXM1 occupancy (**Figure 8C**). Interestingly, we observed a larger size of NCOR1 in the PDA-treated cells compared to the untreated cells (**Figure 8A**). The amount of this larger NCOR1 protein gradually increased with increasing PDA dose (**Figure 8A**). Given that a previous study showed that NCOR1 can be

phosphorylated by the kinase AKT1 [19], we speculated that this larger size band was the phosphorylated NCOR1. To verify this possibility, we cultured cells in two doses of PDA (0.1 and 0.3 mM), followed by treatment with alkaline phosphatase. The western blotting results indicated that alkaline phosphatase eliminated the larger size of NCOR1 (**Figure 8D**), suggesting it to be phosphorylated NCOR1. Moreover, we also examined PUMA, APAF1 and CASP3/7/9 in these cells. The immunoblot results showed that the induction of PUMA and APAF1 and the activation of caspases could all be eliminated by alkaline phosphatase (**Figure 8D** and Supplementary Figure 5). These results suggested that AKT1-mediated phosphorylation of NCOR1 was required for the activation of apoptosis signaling. To further solidify this conclusion, we first examined the protein level of AKT1 in cells treated with different dosages of PDA. We found that AKT1 was dose-dependently increased following PDA treatments (**Figure 8E**). Next, we generated an AKT1-KD cell line and examined whether PDA could still induce apoptosis in AKT-KD cells. Following 0.3 mM PDA treatment, AKT1 protein could be induced to a level comparable to that of the Control-KD cells without PDA treatment, but it was much lower than that of the Control-KD cells induced by PDA (**Figure 8F** and Supplementary Figure 6). Interestingly, the NCOR1 protein level was not changed in PDA-treated AKT1-KD cells compared to untreated cells (**Figure 8F** and Supplementary Figure 6). Importantly, the pro-apoptotic proteins PUMA, APAF1 and caspases were not activated by PDA in the AKT1-KD cells (**Figure 8F** and Supplementary Figure 6). Using these cells, we also performed ChIP assays with anti-FOXM1, anti-NCOR1 and IgG. The occupancies of FOXM1 and NCOR1 were unchanged in the PDA-treated AKT1-KD cells compared to untreated cells (Supplementary Figure 7). These results supported our conclusion that the failed phosphorylation of NCOR1 after PDA treatment resulted in no activation of apoptosis signaling.

Discussion

Apoptosis is an important process that leads to muscle degeneration in the pathogenesis of sarcopenia [17]. A variety of exogenous and endogenous stimuli, such as growth factor deprivation, DNA damage, viral invasion, ischemia, and oxidative stress, can trigger apoptosis [11, 20]. LCFAs mainly function in two aspects: as structural components of cellular membranes and as energy store in triacylglycerols [21, 22]. In the present study, we found that the aberrant accumulation of LCFAs might be associated with sarcopenia pathogenesis. Our study investigated the *in vitro* effects of PDA, which is the most highly accumulated LCFA in the muscle tissue of sarcopenia patients. We found that PDA could induce AKT1, which phosphorylated the transcription corepressor NCOR1, causing the disassociation of the NCOR1-FOXM1 complex. The released FOXM1 docked onto the promoter of *PUMA* and activated its expression. The induction of PUMA triggered its downstream apoptotic signaling and activated the caspase cascades, leading to cell apoptosis, and eventually causing sarcopenia pathogenesis (**Figure 9**).

Aging can induce changes in fat metabolism, causing the increased deposition of fat in non-adipose tissues, including skeletal muscles [23, 24]. Several interesting studies have shown that the increase of intramuscular lipid may result in lipotoxicity, compromising muscle proteins and inducing inflammation [6-8]. LCFAs, such as palmitic acid and oleic acid, have been reported to induce apoptosis in a previous study [6]. In astrocytes, palmitic acid can induce autophagy and cause the degradation of Cav-1, an important protein that controls astrocyte survival [10]. Feeding a high-fat diet causes Cav-1 degradation and leads to apoptosis and inflammation in the hippocampal astrocytes of rats [10]. In some cancer types, oleic acid represses the expression of cyclin D1 and BCL2 but activates the p53-dependent apoptotic signaling pathway [25-27]. However, remains unknown whether LCFAs contribute to apoptosis in the pathogenesis of sarcopenia. We found three LCFAs, PDA, stearic acid and palmitic acid, to be significantly accumulated in muscle tissue samples from sarcopenia patients (**Figure 1**). Although we only investigated the role of PDA in sarcopenia pathogenesis, we cannot exclude the other two LCFAs from also contributing to this process. Our findings are considerably different from a previous report that showed linoleic acid, stearic acid, and vaccenic acid to be accumulated in the quadriceps muscle from rats that were fed a

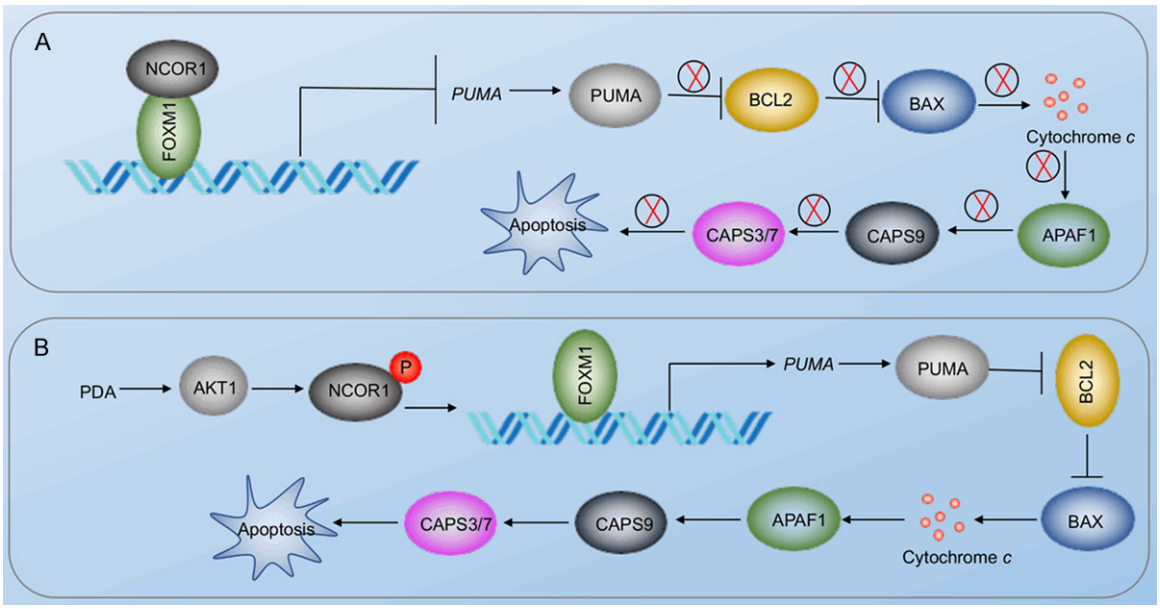

Figure 9. A schematic diagram of PDA-activated apoptosis signaling in the pathogenesis of sarcopenia. A. Schematic diagram of the NCOR1-FOXM1 transcriptional complex in non-sarcopenic muscles. The NCOR1-FOXM1 complex docks on the promoter of *PUMA*, and NCOR1 functions as a repressor to inhibit the expression of *PUMA*. The repression of PUMA inhibits its downstream molecules, such as BAX, APAF1, and CASP3/7/9. B. Schematic diagram of PDA-mediated signaling. The accumulation of PDA activates AKT1, causing the phosphorylation of NCOR1. The phosphorylated NCOR1 fails to assemble a complex with FOXM1, leading to the upregulation of *PUMA*. The induction of PUMA initiates its downstream apoptosis signaling, leading to cell apoptosis and the pathogenesis of sarcopenia.

high-fat diet [6]. These differences suggest that the metabolism and deposition of LCFAs in humans and rats may be quite distinct due to the different diets. In addition, our microarray results showed that several proinflammatory cytokine genes (*IL-1B*, *IL-6* and *TNFA*) were dose-dependently induced in PDA-treated cells (**Figure 2A**); however, we did not investigate whether AKT1-mediated signaling contributed to their induction. Given that inflammation is also an important contributor to sarcopenia pathogenesis, future studies should investigate the molecular mechanism by which PDA induces the expression of proinflammatory cytokine genes. This information would help clarify how PDA accumulation contributes to sarcopenia pathogenesis.

Several studies have shown that the autophagic degradation of FOXO3a, a homolog of FOXM1, can regulate *PUMA* expression to mediate apoptosis in different cancers [15, 16]. In the current study, we found the significant induction of FOXM1, but not of FOXO3a, in PDA-treated cells. Unlike previous studies, we found that NCOR1 and FOXM1 form a transcriptional complex to regulate *PUMA* expression. In normal cells, unphosphorylated NCOR1 can negatively regulate FOXM1-mediated transcription. When PDA accumulates in sarcopenic muscles, it can activate AKT1 and cause NCOR1 to become phosphorylated. This results in the disassociation of the NCOR1-FOXM1 complex, leading to the activation of PUMA and its downstream signals. Our research further elucidates the regulatory mechanisms of the FOX family proteins. To our knowledge, this is the first report showing that FOXM1 and other FOX family members have this unique mode of regulation. Although we clearly demonstrated this signaling *in vitro*, future *in vivo* work is required to characterize the effects of PDA on AK1/NCOR1/FOXM1-mediated apoptotic signaling in animal models.

In conclusion, we revealed that the accumulation of PDA in sarcopenic muscle tissues can cause apoptosis. *In vitro* analyses demonstrated that PDA activates AKT1, which phosphorylates NCOR1, causing the release of FOXM1 from the NCOR1-FOXM1 transcriptional complex. FOXM1 induces the expression of *PUMA* through a p53-independent mechanism. The activation of PUMA initiates its downstream

apoptotic signaling. The detailed description of this signaling suggests that decreasing the intake of PDA-containing food and blocking AKT1 kinase activity may be two potential strategies to improve sarcopenic outcomes.

Acknowledgements

We would like to thank muscle tissue donors for this study. This work was supported by a grant from the Department of Science and Technology, Jiangxi Province, China (No. 20161BBG70131).

Disclosure of conflict of interest

None.

Address correspondence to: Dr. Le Peng, Department of Geriatrics, Jiangxi Provincial People's Hospital Affiliated to Nanchang University, No. 92 Aiguo Road, Nanchang 330006, Jiangxi, China. E-mail: le.peng2010@gmail.com

References

[1] Santilli V, Bernetti A, Mangone M and Paoloni M. Clinical definition of sarcopenia. Clin Cases Miner Bone Metab 2014; 11: 177-180.

[2] Ogawa S, Yakabe M and Akishita M. Age-related sarcopenia and its pathophysiological bases. Inflamm Regen 2016; 36: 17.

[3] Kalyani RR, Corriere M and Ferrucci L. Age-related and disease-related muscle loss: the effect of diabetes, obesity, and other diseases. Lancet Diabetes Endocrinol 2014; 2: 819-829.

[4] Walewski JL, Ge F, Gagner M, Inabnet WB, Pomp A, Branch AD and Berk PD. Adipocyte accumulation of long-chain fatty acids in obesity is multifactorial, resulting from increased fatty acid uptake and decreased activity of genes involved in fat utilization. Obes Surg 2010; 20: 93-107.

[5] Walle P, Takkunen M, Mannisto V, Vaittinen M, Kakela P, Agren J, Schwab U, Lindstrom J, Tuomilehto J, Uusitupa M and Pihlajamaki J. Alterations in fatty acid metabolism in response to obesity surgery combined with dietary counseling. Nutr Diabetes 2017; 7: e285.

[6] Laurentius T, Kob R, Fellner C, Nourbakhsh M, Bertsch T, Sieber CC and Bollheimer LC. Long-chain fatty acids and inflammatory markers coaccumulate in the skeletal muscle of sarcopenic old rats. Dis Markers 2019; 2019: 9140789.

[7] Kob R, Bollheimer LC, Bertsch T, Fellner C, Djukic M, Sieber CC and Fischer BE. Sarcopenic obesity: molecular clues to a better understanding of its pathogenesis? Biogerontology 2015; 16: 15-29.

[8] Collins KH, Paul HA, Hart DA, Reimer RA, Smith IC, Rios JL, Seerattan RA and Herzog W. A high-fat high-sucrose diet rapidly alters muscle integrity, inflammation and gut microbiota in male rats. Sci Rep 2016; 6: 37278.

[9] Lee JY, Sohn KH, Rhee SH and Hwang D. Saturated fatty acids, but not unsaturated fatty acids, induce the expression of cyclooxygenase-2 mediated through Toll-like receptor 4. J Biol Chem 2001; 276: 16683-16689.

[10] Chen Z, Nie SD, Qu ML, Zhou D, Wu LY, Shi XJ, Ma LR, Li X, Zhou SL, Wang S and Wu J. The autophagic degradation of Cav-1 contributes to PA-induced apoptosis and inflammation of astrocytes. Cell Death Dis 2018; 9: 771.

[11] Elmore S. Apoptosis: a review of programmed cell death. Toxicol Pathol 2007; 35: 495-516.

[12] Zhang F, Zhao X, Shen H and Zhang C. Molecular mechanisms of cell death in intervertebral disc degeneration (review). Int J Mol Med 2016; 37: 1439-1448.

[13] Yuan Z, Cao K, Lin C, Li L, Liu HY, Zhao XY, Liu L, Deng HX, Li J, Nie CL and Wei YQ. The p53 upregulated modulator of apoptosis (PUMA) chemosensitizes intrinsically resistant ovarian cancer cells to cisplatin by lowering the threshold set by Bcl-x(L) and Mcl-1. Mol Med 2011; 17: 1262-1274.

[14] You H, Pellegrini M, Tsuchihara K, Yamamoto K, Hacker G, Erlacher M, Villunger A and Mak TW. FOXO3a-dependent regulation of Puma in response to cytokine/growth factor withdrawal. J Exp Med 2006; 203: 1657-1663.

[15] Fitzwalter BE, Towers CG, Sullivan KD, Andrysik Z, Hoh M, Ludwig M, O'Prey J, Ryan KM, Espinosa JM, Morgan MJ and Thorburn A. Autophagy inhibition mediates apoptosis sensitization in cancer therapy by relieving FOXO3a turnover. Dev Cell 2018; 44: 555-565, e3.

[16] Jiang K, Zhang C, Yu B, Chen B, Liu Z, Hou C, Wang F, Shen HX and Chen Z. Autophagic degradation of FOXO3a represses the expression of PUMA to block cell apoptosis in cisplatin-resistant osteosarcoma cells. Am J Cancer Res 2017; 7: 1407-1422.

[17] Chen FX, Shen Y, Liu Y, Wang HF, Liang CY and Luo M. Inflammation-dependent downregulation of miR-532-3p mediates apoptotic signaling in human sarcopenia through targeting BAK1. Int J Biol Sci 2020; 16: 1481-1494.

[18] Bulynko YA and O'Malley BW. Nuclear receptor coactivators: structural and functional biochemistry. Biochemistry 2011; 50: 313-328.

[19] Jo YS, Ryu D, Maida A, Wang X, Evans RM, Schoonjans K and Auwerx J. Phosphorylation

of the nuclear receptor corepressor 1 by protein kinase B switches its corepressor targets in the liver in mice. Hepatology 2015; 62: 1606-1618.
[20] Redza-Dutordoir M and Averill-Bates DA. Activation of apoptosis signalling pathways by reactive oxygen species. Biochim Biophys Acta 2016; 1863: 2977-2992.
[21] Schonfeld P and Wojtczak L. Short- and medium-chain fatty acids in energy metabolism: the cellular perspective. J Lipid Res 2016; 57: 943-954.
[22] de Carvalho CCCR and Caramujo MJ. The various roles of fatty acids. Molecules 2018; 23: 2583.
[23] Carter CS, Justice JN and Thompson L. Lipotoxicity, aging, and muscle contractility: does fiber type matter? Geroscience 2019; 41: 297-308.
[24] Tchkonia T, Morbeck DE, Von Zglinicki T, Van Deursen J, Lustgarten J, Scrable H, Khosla S, Jensen MD and Kirkland JL. Fat tissue, aging, and cellular senescence. Aging Cell 2010; 9: 667-684.
[25] Jiang L, Wang W, He Q, Wu Y, Lu Z, Sun J, Liu Z, Shao Y and Wang A. Oleic acid induces apoptosis and autophagy in the treatment of Tongue Squamous cell carcinomas. Sci Rep 2017; 7: 11277.
[26] Ma S, Chen F, Ye X, Dong Y, Xue Y, Xu H, Zhang W, Song S, Ai L, Zhang N and Pan W. Intravenous microemulsion of docetaxel containing an anti-tumor synergistic ingredient (brucea javanica oil): formulation and pharmacokinetics. Int J Nanomedicine 2013; 8: 4045-4052.
[27] Shaikh IA, Brown I, Wahle KW and Heys SD. Enhancing cytotoxic therapies for breast and prostate cancers with polyunsaturated fatty acids. Nutr Cancer 2010; 62: 284-296.

Supplementary Table 1. Primers used for RT-qPCR analyses to examine gene expression levels

Gene	Forward Primers (5'→3')	Reverse primers (5'→3')
FOXM1	TGTGCTCAAGCTGTCCACCATCC	ACACAAGGTCCCAGCAGTGGC
PUMA	GACTTTCTCTGCACCATGTAGCA	GTCCCTCTCCTGGCTTCTTGGCCAG
APAF1	TCACAGCACCATCCAGTACTG	CCCAACTTAAATGTCCTCTGCAAT
KAT5	TGTTTGGGCACTGATGAGGACT	CTCAATGCACTCAATGTTCTTCA
MSH6	GATTAGACAGTGTTCCAGCACC	ATCAGGGACATGATGTAGAG
BCL2	CCAGAGACATCAGCATGGCTC	GATGTCCCTACCAACCAGAAG
BIRC5	GTCTGTCAGCCCAACCTTCAC	ACCCTGCAGCTCTATGACAG
NPM1	GGAAGATGCAGAGTCAGAAGA	TCCTCTTCATCATCATCGTCA
NOD1	GCAGATGCGTTACAGAGCAACA	GAAACAGATAATCCGCTTCTC
FAS	GGCAAGACTGCCCTTAGAAAT	AGCAGGTTTTACATGGGACAT
TRADD	TGGAGGCACTCGAGGAGAACGA	AGGAACCCTAAGGCCATCCA
P53	AAGGGCCTGACTCAGACTGAC	GAAGTCCTGGGTGCTTCTGAC
BIM	GTGTGGAGAATGCATTGACAG	CTGAAACGTCACCTGCCCCCT
BAX	TCTGAGCAGATCATGAAGACA	ACACTCGCTCAGCTTCTTGGTG
BAK1	AGATGGTCACCTTACCTCTGCA	TTCTCTGCCGTGGGCTGCAGGT
NCOR1	GGGTCTTAAGCTATTCTGAGT	AGGCTGAGGATGAGAAGGGGTT
β-Actin	CAGGTCATCACCATTGGCAAT	GTCTTTGCGGATGTCCACGTCA

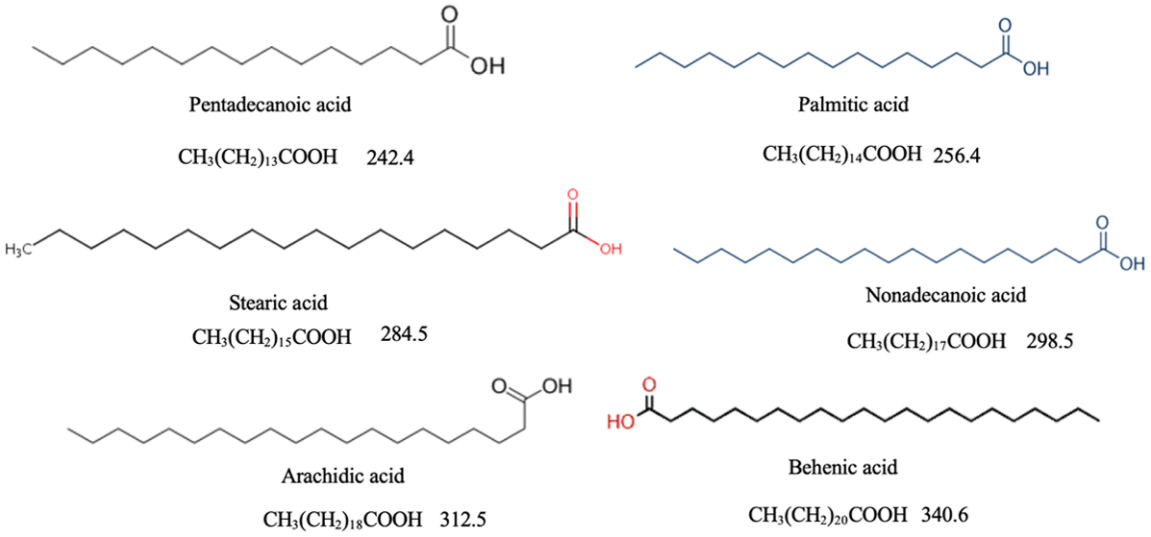

Supplementary Figure 1. The chemical structures of LCFAs identified by GC-MS. The chemical structures of six LCFAs (PDA, stearic acid, palmitic acid, nonadecanoic acid, arachidic acid and behenic acid) as shown in **Figure 1** and their molecular weights.

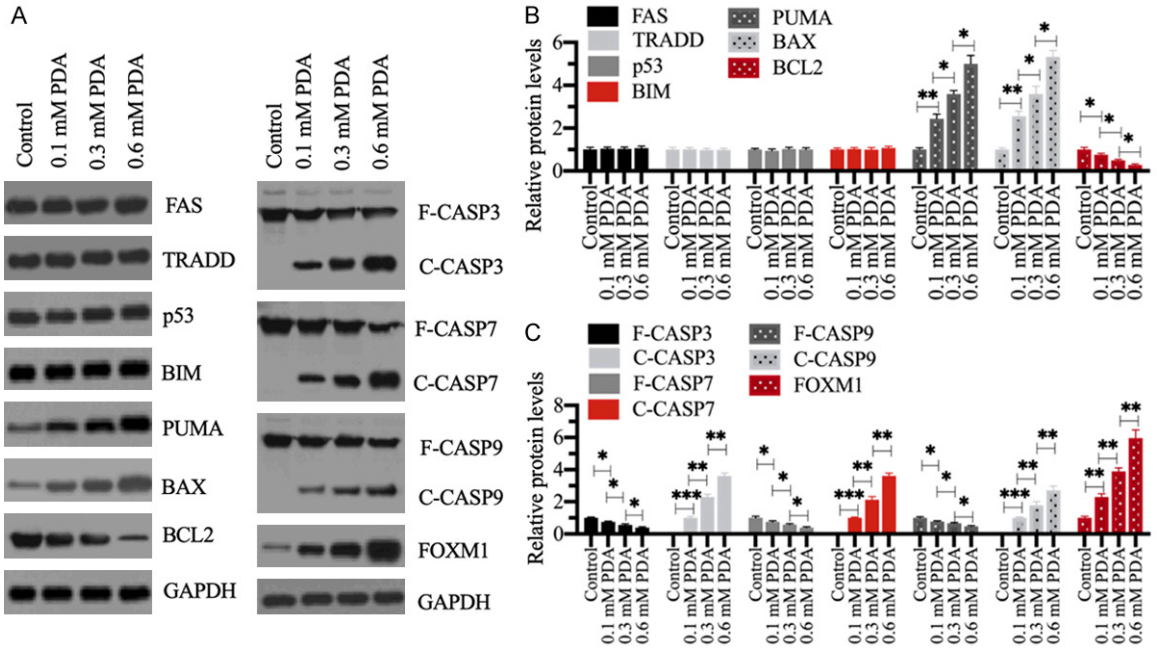

Supplementary Figure 2. The protein levels of genes involved in apoptotic signaling in PDA-treated cells. A. Immunoblot results. Total cell extracts from cells treated with different doses of PDA (0, 0.1, 0.3 and 0.6 mM) were subjected to western blotting to examine the protein levels of FAS, TRADD, p53, BIM, PUMA, BAX, BCL2, CASP3, CASP7, CASP9, and FOXM1. F: full length; C: cleaved form. B and C. Quantification of protein band signals. The protein band signals in A were quantified using Image J software. Statistical significance is denoted by * for $P<0.05$, ** for $P<0.01$, and *** for $P<0.001$.

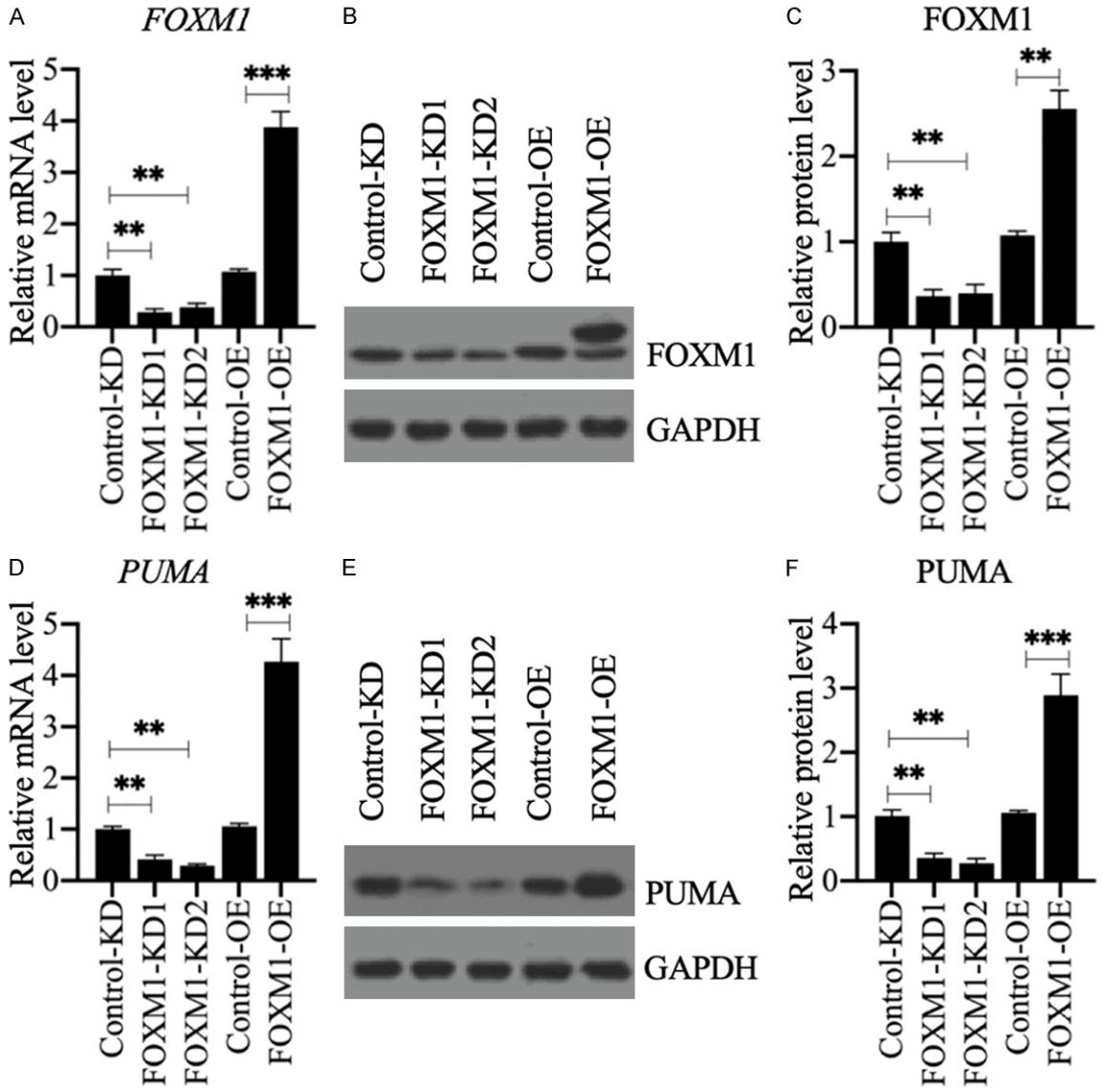

Supplementary Figure 3. The effects of *FOXM1* knockdown and overexpression on PUMA expression. (A) The relative mRNA level of *FOXM1*. Total RNA from Control-KD, FOXM1-KD1, FOXM1-KD2, Control-OE, and FOXM1-OE1 cells was applied to RT-qPCR analysis to examine the *FOXM1* mRNA level. ***P*<0.01 and ****P*<0.001. (B and C) The protein level of FOXM1. Total cell extracts from cells used in (A) were applied to western blotting to examine the protein levels of FOXM1 and GAPDH (loading control) (B). The FOXM1 protein signals were quantified using ImageJ software and normalized to their corresponding GAPDH levels (C). ***P*<0.01. (D) The relative *PUMA* mRNA level. The same RNA samples as used in (A) were subjected to RT-qPCR analysis to examine the expression of *PUMA*. ***P*<0.01 and ****P*<0.001. (E and F) PUMA protein levels. The same cell extracts as used in (B) were applied to western blotting to examine the protein levels of PUMA and GAPDH (loading control) (E). The PUMA protein signals were quantified using ImageJ software and normalized to their corresponding GAPDH levels (F). ***P*<0.01 and ****P*<0.001.

Supplementary Table 2. The FOXM1-associated proteins by LC-MS/MS analysis

Protein	Protein description	Percolator score	Molecular weight
FOXM1	Forkhead Box M1	7436	84283
NPM1	Nucleophosmin 1	65543	32575
NRIP2	Nuclear Receptor Interacting Protein 2	5231	31331
KIF2A	Kinesin Family Member 2A	5012	79955
HSPA4	Heat Shock Protein Family A (Hsp70) Member 4	4657	94331

UHRF1	Ubiquitin Like With PHD And Ring Finger Domains 1	4332	89814
IFI27	Interferon Alpha Inducible Protein 27	3678	11542
RRM1	Ribonucleotide Reductase Catalytic Subunit M1	3212	90070
PPP2CA	Protein Phosphatase 2 Catalytic Subunit Alpha	3094	35594
PCLAF	PCNA Clamp Associated Factor	2778	11986
RPA2	Replication Protein A2	2543	29247
SPC25	SPC25 Component Of NDC80 Kinetochore Complex	2123	26153
SMC4	Structural Maintenance Of Chromosomes 4	2094	147182
NSCAN12	Zinc Finger And SCAN Domain Containing 12	1965	70222
DMAP1	DNA Methyltransferase 1 Associated Protein 1	1932	52993
MKS1	MKS Transition Zone Complex Subunit 1	1902	64528
CALM2	Calmodulin 2	1854	16838
PIGL	Phosphatidylinositol Glycan Anchor Biosynthesis Class L	1823	28531
NCOR1	Nuclear Receptor Corepressor 1	1793	270210
NR1D2	Nuclear Receptor Subfamily 1 Group D Member 2	1744	64625
SIAH2	Siah E3 Ubiquitin Protein Ligase 2	1732	34615
TBL1X	Transducin Beta Like 1 X-Linked	1657	62496
MECP2	Methyl-CpG Binding Protein 2	1432	52441
PRMT1	Protein Arginine Methyltransferase 1	1335	42462
BAZ1A	Bromodomain Adjacent To Zinc Finger Domain 1A	1207	178702
PLD6	Phospholipase D Family Member 6	1184	28273
BAZ2A	Bromodomain Adjacent To Zinc Finger Domain 2A	1034	211198
TEKT3	Tektin 3	1021	56636
PBRM1	Polybromo 1	968	192948
DDX20	DEAD-Box Helicase 20	903	92241
MED19	Mediator Complex Subunit 19	887	26273
ERBB2	Erb-B2 Receptor Tyrosine Kinase 2	834	137910
DDX46	DEAD-Box Helicase 46	812	117362
EWSR1	EWS RNA Binding Protein 1	789	68478
RPS11	Ribosomal Protein S11	764	18431
MED9	Mediator Complex Subunit 9	692	16403
POLR1C	RNA Polymerase I And III Subunit C	632	39250
DVL2	Dishevelled Segment Polarity Protein 2	587	78948
DAP3	Death Associated Protein 3	532	45566
TAF9	TATA-Box Binding Protein Associated Factor 9	511	28974
CORO2A	Coronin 2A	489	59763
CDRT4	CMT1A Duplicated Region Transcript 4	463	17643
NR2C1	Nuclear Receptor Subfamily 2 Group C Member 1	411	67315
DUS3L	Dihydrouridine Synthase 3 Like	406	72594
MTMR3	Myotubularin Related Protein 3	394	133619
XPO5	Exportin 5	365	136311
NUP160	Nucleoporin 160	342	162121
FLNA	Filamin A	322	280739
H2BC5	H2B Clustered Histone 5	312	13936
UPF1	UPF1 RNA Helicase And ATPase	287	124345
SMYD3	SET And MYND Domain Containing 3	265	49097
SND1	Staphylococcal Nuclease And Tudor Domain Containing 1	243	101997
MYL6	Myosin Light Chain 6	225	16930
SCAP	SREBF Chaperone	212	139729

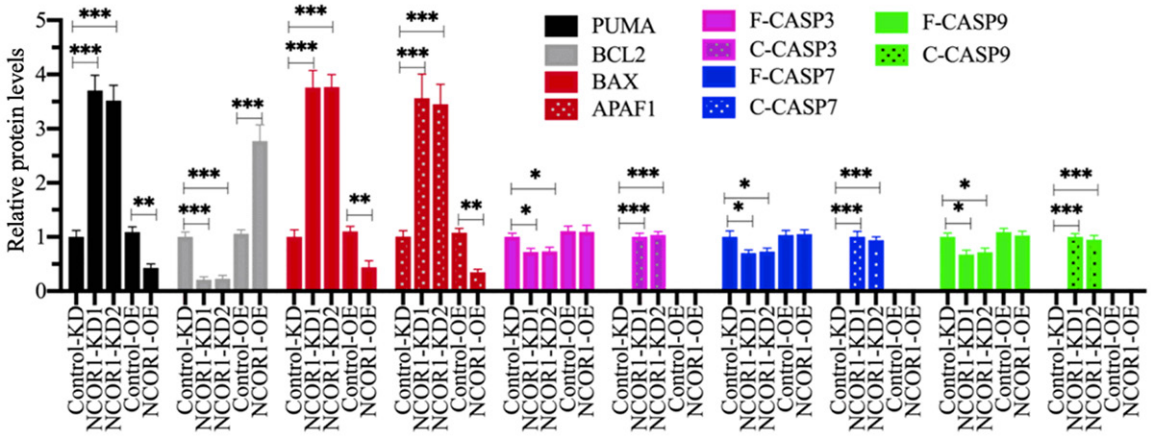

Supplementary Figure 4. The relative protein levels of apoptotic proteins in NCOR1-KD cells. The protein signals shown in **Figure 7F** were quantified using ImageJ software and normalized to their corresponding GAPDH level. **P*<0.05, ***P*<0.01 and ****P*<0.001.

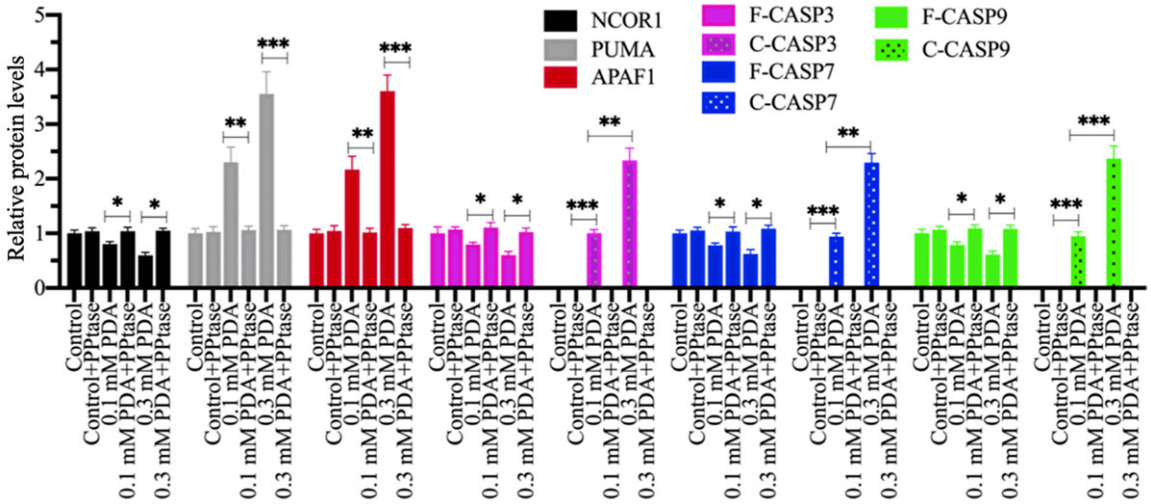

Supplementary Figure 5. The relative protein levels of apoptotic proteins in cells treated with or without PDA and PPtase. The protein signals shown in **Figure 8D** were quantified using ImageJ software and normalized to their corresponding GAPDH level. **P*<0.05, ***P*<0.01 and ****P*<0.001.

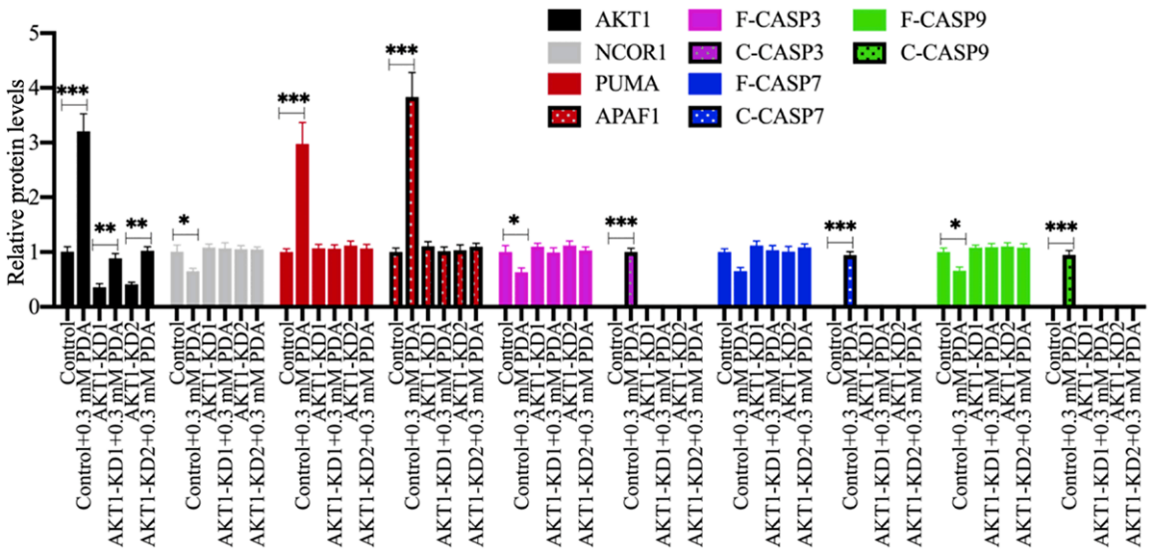

Supplementary Figure 6. The relative protein levels of apoptotic proteins in AKT-KD cells treated with or without PDA. The protein signals shown in **Figure 8F** were quantified using ImageJ software and normalized to their corresponding GAPDH level. **P*<0.05, ***P*<0.01 and ****P*<0.001.

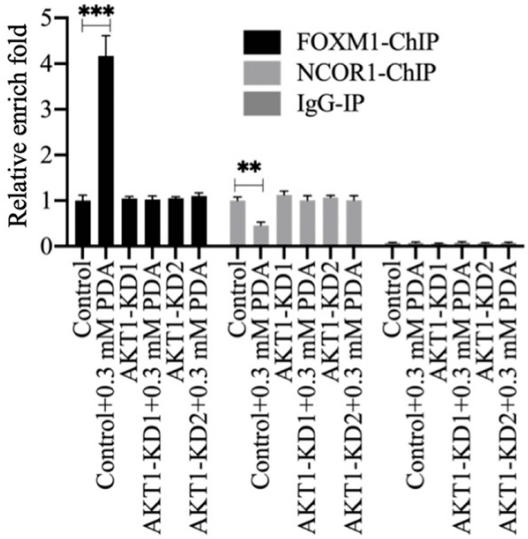

Supplementary Figure 7. The occupancies of NCOR1 and FOXM1 on the promoter of *PUMA*. Cells used in **Figure 8F** were subjected to ChIP assays using anti-NCOR1, anti-FOXM1 and IgG (negative control). The purified input and output DNA samples were subjected to RT-qPCR analysis to examine the occupancy of NCOR1 and FOXM1 on the promoter of *PUMA*. ***P*<0.01 and ****P*<0.001.